JACS
JOURNAL OF THE AMERICAN CHEMICAL SOCIETY

Communication

pubs.acs.org/JACS

Electrochemical (De)Lithiation of 1D Sulfur Chains in Li–S Batteries: A Model System Study

Chun-Peng Yang,[†,‡] Ya-Xia Yin,[†] Yu-Guo Guo,*[,†] and Li-Jun Wan*[,†]

[†]CAS Key Laboratory of Molecular Nanostructure and Nanotechnology and Beijing National Laboratory for Molecular Sciences, Institute of Chemistry, Chinese Academy of Sciences (CAS), Beijing 100190, P. R. China

[‡]University of Chinese Academy of Sciences, Beijing 100049, P. R. China

Supporting Information

ABSTRACT: In contrast to the extensive studies of the electrochemical behavior of conventional cyclic S_8 molecules in Li–S batteries, there has been hardly any investigation of the electrochemistry of S chains. Here we use S chains encapsulated in single- and double-walled carbon nanotubes as a model system and report the electrochemical behavior of 1D S chains in Li–S batteries. An electrochemical test shows that S chains have high electrochemical activity during lithiation and extinctive electrochemistry compared with conventional S_8. The confined steric effect provides Li^+ solid-phase diffusion access to insert/egress reactions with S chains. During lithiation, the long S chains spontaneously become short chains, which show higher discharge plateaus and better kinetics. The unique electrochemistry of S chains supplements the existing knowledge of the S cathode mechanism and provides avenues for rational design of S cathode materials in Li–S batteries.

Increasing needs for renewable energy have spurred tremendous efforts on the investigation of advanced electrochemical energy storage materials.[1] Because of its high capacity, low cost, and abundance, the use of sulfur as a cathode for rechargeable metallic batteries (lithium, sodium, and magnesium batteries) has long fascinated the scientific community.[2] In the past few decades, intensive research has greatly improved the battery performance of Li–S batteries, making their practical applications possible; however, issues still remain.[3] Meanwhile, theoretical studies of the electrochemistry of Li–S batteries have gained great achievement as well.[4] Special interest has been devoted to the electrochemical reaction mechanism of orthorhombic α-S_8, as it is the most stable allotrope of S and widely used in current Li–S batteries.[3b] The two-plateau reaction mechanism involving polysulfide intermediates (Li_2S_x, x = 2–8) is now well-known and provides theoretical guidance in designing advanced S cathodes. Small S molecules confined in micropores (S_{2-4}), revealed by our earlier research, show different electrochemistry without high-order polysulfide intermediates (S_n^{2-}, n = 6–8) and therefore exceptional electrochemical performance.[2c,5] Monoclinic β-S_8 exhibits special performance as well.[6] Unremitting efforts to explore new S allotropes with distinctive electrochemical behavior will open additional avenues for the future of S cathode materials.

Sulfur is the element with the most numerous solid allotropic forms. At present, there are approximately 30 known S allotropes, which are composed of rings or chains.[7] The ring structures, particularly cyclic S_8, have been widely investigated. Allotropes consisting of chains, however, are less well characterized, and their electrochemistry has rarely been investigated. In fact, chain structures could be more interesting for batteries in comparison with rings, as the former are very electrochemically active.[8] Chainlike S allotropes could be a new kind of S cathodes and deserve more attention. A comprehensive study of the electrochemistry of S chains in Li–S batteries is therefore considerably important and will facilitate the future development of cathode materials based on S chains. However, as S chains usually coexist with S_8 rings,[7a,c] electrochemical studies of S chains using conventional S chain allotropes inevitably suffer from interference by S_8 rings.

Recently Fujimori et al.[9] reported that S can be isolated inside single-walled and double-walled carbon nanotubes (SWCNTs and DWCNTs, collectively called CNTs) as unambiguous one-dimensional (1D) chains. The S chains are stable because of the spatial confinement and are electronically conducting because of the reduced dimension. This structure is completely different from that of S with multiwalled carbon nanotubes, where the S is composed of S_8 rings.[10] Well-defined 1D S chains encapsulated in CNTs (S/CNTs) provide an ideal model system to investigate the electrochemical (de)lithiation processes of S chains, as the system is stable and easy to observe during reactions. In this work, we used S/CNTs as a model system to gain insight into the electrochemical (de)lithiation behavior of S chains. We found that S chains display a high electrochemical activity and undergo a solid-phase electrochemical reaction. The intrinsic electrochemical nature of S chains revealed by the model system is independent of the specific system and paves the way for the applications of S chains in energy storage systems.

S/CNTs were synthesized via the method described by Fujimori et al.[9] The pronounced Bragg peaks of S/CNTs in the powder X-ray diffraction (XRD) pattern (Figure 1a) indicate long-range order of the S atoms. These peaks have already been indexed as the characteristic peaks of 1D sulfur chains. The 1D structure can be observed from the high-resolution transmission electron microscopy (HRTEM) image (Figure 1a inset). This is significantly different from bulk S crystals (α-S_8 and β-S_8) and is in contrast to S molecules confined in microporous carbon,

Received: December 22, 2014
Published: February 4, 2015

DOI: 10.1021/ja513009v
J. Am. Chem. Soc. 2015, 137, 2215–2218

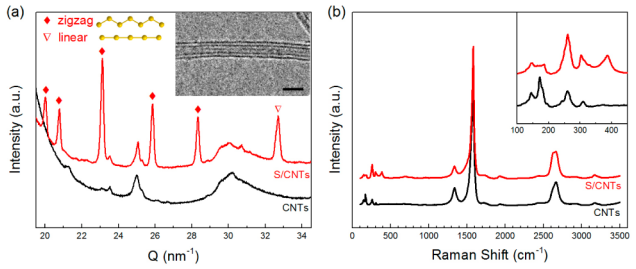

Figure 1. (a) XRD profiles of CNTs and S/CNTs. The inset shows a 1D S chain in a DWCNT (scale bar 2 nm). (b) Raman spectra of CNTs and S/CNTs. The inset shows the RBM region.

where S is amorphous.[5] In agreement with the results of Fujimori et al.,[9] the peak at a scattering vector (Q) of 32.8 nm^{-1} is associated with a lattice constant (d) of 0.192 nm, approaching the S–S bond length (0.189–2.066 nm in S allotropes[7c]), and is therefore attributed to linear chains. Other peaks, aside from the characteristic peaks of CNTs, are assigned to different types of zigzag S chains. The linear and zigzag S chains depend on the inner diameter of the CNTs and can be distinguished from the Bragg peaks. The Raman spectrum of S/CNTs displays an extra peak at 390 cm^{-1} in addition to the radial breathing mode (RBM) peaks of CNTs[11] (Figure 1b). This peak at 390 cm^{-1} is not observed in CNTs and should be attributed to the S chains. This result is also in accordance with the report of Fujimori et al.,[9] further confirming the 1D S chains inside CNTs. In addition, neither characteristic XRD peaks nor Raman peaks of α-S (Figure S1) were identified in S/CNTs, indicating that all of the sulfur is encapsulated in CNTs as S chains with uniform distribution (Figure S2). The S content is 12.4 wt % according to the C–S elemental analysis, confirmed by quantitative analysis using an electron probe microanalyzer (Figure S3).

The electrochemistry of S/CNTs was investigated as the model of S chains. As shown by the galvanostatic discharge/charge voltage profile at 0.1 C (Figure 2a), S/CNTs deliver a high discharge capacity approaching 2000 mA h g^{-1}. We note that during discharge to 1.0 V, the CNTs also contribute part of the capacity (Figure S4). The initial capacity of S after deduction

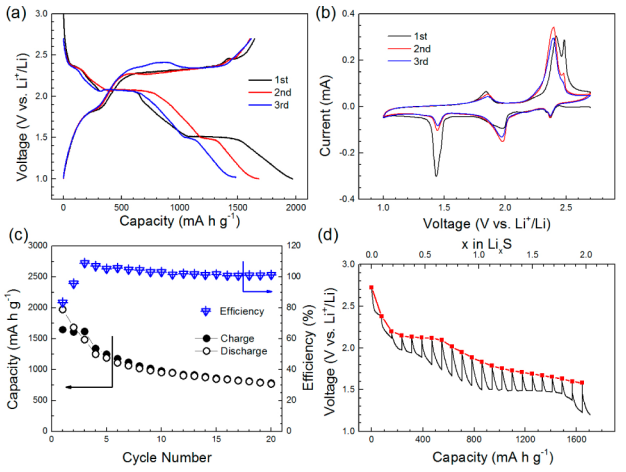

Figure 2. (a) Galvanostatic discharge/charge voltage profiles of S/CNTs tested at 0.1 C (based on S). (b) CVs of S/CNTs in the initial three cycles at a scan rate of 0.1 mV/s. (c) Capacity and Coulombic efficiency of S/CNTs at 0.1 C. (d) GITT profile of S/CNTs during the initial discharge at 0.1 C. The OCV is marked by the red line.

of the contribution of CNTs (based on the initial capacity of the CNTs and the content of C in S/CNTs), is ~1500 mA h g^{-1}, which is slightly less than the theoretical capacity of S (1675 mA h g^{-1}). The high capacity reflects the high electrochemical activity of S chains. When charged, Li^+ ions are able to take off from S/CNTs reversibly. There is a noticeable discharge plateau at 1.45 V in the discharge/charge curve, consistent with the cyclic voltammogram (CV) (Figure 2b). The discharge voltage of 1.45 V is rarely observed in conventional Li–S batteries and is a distinct discharge feature of 1D S chains confined in CNTs. The intensity of the reduction peak at 1.45 V is reduced in the ensuing cycles, but the broad peak at 2.0 V increases, possibly indicating structural evolution during cycling. After 20 cycles, S/CNTs show a stable reversible capacity of ~800 mA h g^{-1} (Figure 2c). The Coulombic efficiency is ~100%, indicating that the shuttle effect is negligible because of the confinement of CNTs. This can be further proved by checking the cycled anode and cathode (Figures S5–S7).

The galvanostatic intermittent titration technique (GITT) was applied to determine the quasi-equilibrium reduction potential (quasi-open circuit potential, OCV) of S chains (Figure 2d). The reduction of S chains at the equilibrium state takes place with a plateau at 2.1 V and a slope around 1.8 V. The OCV curve exhibits the electrochemical characteristic of the S chains, which is different from that of S_8 molecules. The OCV is ~0.3 V higher than the nonequilibrium discharge voltage, reflecting slow kinetics. The kinetic process is limited by Li^+ diffusion through the CNTs with a high aspect ratio. Therefore, the discharge voltages in Figure 2a result from the thermodynamic nature of S chains and the kinetic limitations of CNTs. With improved kinetics, the output voltage is expected to improve to 2.1 and 1.8 V. The output plateaus are slightly higher than that of S molecules in micropores[5] and are feasible for use as Li–S battery cathodes. Although the above results were measured in an ether-based electrolyte, the electrochemical lithiation of S chains in carbonate-based electrolytes shares much in common, research on which is still in progress.

To identify the composition of the intermediate products during electrochemical reaction, S/CNT electrodes were analyzed by ex situ X-ray photoelectron spectroscopy (XPS). The S $2p_{3/2}$ and $2p_{1/2}$ dual peaks of pristine S/CNTs (Figure 3a) at 164.1 and 165.2 eV were almost identical to those of pure S (Figure S8), except for the small amount S/CNTs oxidation species at ~169 eV. During electrochemical reaction, several S species were probed by XPS (Figure 3b,c). The peaks in the high-binding-energy region (166–172 eV) are attributed to oxidized S

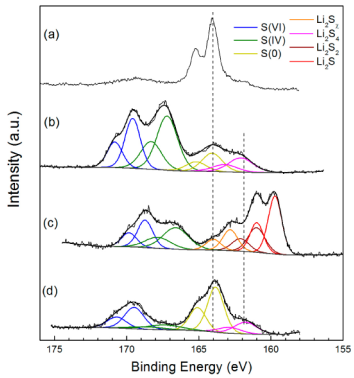

Figure 3. Ex situ XPS spectra of S 2p in S/CNTs: (a) pristine; (b) discharged to 1.8 V; (c) discharged to 1.0 V; (d) recharged to 2.7 V.

DOI: 10.1021/ja513009v
J. Am. Chem. Soc. 2015, 137, 2215–2218

species, which originate from the byproducts.[3g,4c,12] According to the ex situ XPS spectra, upon discharge to 1.8 V, Li_2S_4 was generated, and no Li_2S_χ ($\chi > 4$) intermediates were observed. The original S chains were also detected, indicating the coexistence of two phases (Li_2S_4 and S chains). Upon further discharge to 1.0 V, S chains and Li_2S_4 were progressively reduced to Li_2S_2 and Li_2S (see Figures S9 and S10 for more detailed XPS analyses), exhibiting a sharp reduction peak at 1.45 V (Figure 2b). Additionally, a small portion of Li_2S_χ was observed in the final reduction product, originating from S chains deep in the long CNTs that were not completely reduced. There are possibly more than eight S atoms in Li_2S_χ because it is reduced from long S chains. This is different from the reduction mechanism of conventional S_8 rings. When charged to 2.7 V, the cycled S/CNTs display a binding energy close to the pristine one, indicating that the majority of S species are transformed to elemental S, except a small portion of residual Li_2S_4 (Figure 3d).

Ex situ XRD was conducted to further disclose the crystalline structure evolution of S chains upon electrochemical reaction. XRD profiles of S/CNTs with different depths of reaction (DoR), indicated by points a–g in Figure 4a, were carefully collected at a low scan rate of 0.1° min^{-1} for fine Bragg diffraction peaks. The electrode prior to lithiation was also recorded as the pristine S/CNTs and is marked as point o in Figure 4a. For the zigzag chains, the diffraction peaks (20.1–28.4 nm^{-1} in profiles o–d in Figure 4b) become weak during discharge, indicating a reduction in the domain sizes. In a 1D structure, the domain size ξ is related to the chain length. Therefore, the zigzag chains become short after the initial discharge. Once shortened, most types of the zigzag chains cannot recover the long crystalline structure after one discharge/charge cycle, and their peaks at 20.1, 25.9, and 28.4 nm^{-1} disappear, indicating that the S atoms in these types of chains are no longer ordered. These chains finally become short disordered chains. However, the peak at 23.2 nm^{-1} still exists after one cycle and only becomes weak. This indicates that S atoms in this type of zigzag chain are still crystalline while the domain size is reduced. Therefore, according to the above qualitative analysis for zigzag chains after one cycle, the zigzag chains become short (disordered or crystalline).

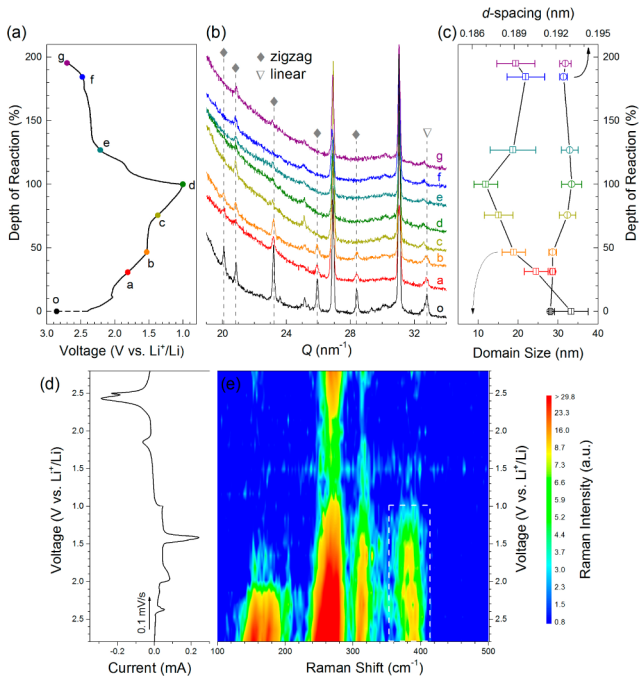

Figure 4. (a) Discharge/charge curve indicating DoR for ex situ analysis. (b) Ex situ XRD at different DoR indicated in (a). The dashes indicate peaks of S chains (the two intense peaks at 26.9 and 31.0 nm^{-1} result from the Al foil and other small peaks result from CNTs). (c) Evolution of domain size and *d*-spacing of linear S chains during lithiation/delithiation. (d) CV of S/CNTs during the initial cycle. (e) Contour plot of Raman spectra of the S/CNT electrode recorded during the initial cycle. The rectangle indicates the characteristic peak of S chains.

In contrast to the zigzag chains, the linear S chains show diffraction peaks during lithiation/delithiation ($Q = 32.8$ nm^{-1} in Figure 4b). Its Q value and full width at half-maximum (ΔQ) change upon lithiation/delithiation. The diffraction *d*-spacing ($d = 2\pi/Q$) and domain size ($\xi = 2\pi/\Delta Q$) of the linear chains were estimated from refined XRD patterns (Figure S11) and are plotted in Figure 4c. With Li^+ intercalation, the S–S distance increases from the pristine value of 0.1916 nm to 0.1931 nm in the final discharge product. Meanwhile, ξ significantly decreases from 33.3 to 11.9 nm, indicating that the length of the S chains is reduced. The S chains cannot completely recover to the original size when Li^+ is extracted from the S chains during charge. When all of the Li^+ ions are egressed (DoR = 200%), ξ of the reformed S chains is ~20 nm, which is much less than the pristine value (33.3 nm). The evolution of linear chains is consistent with the evolution tendency of zigzag chains, i.e., S chains being curtailed to shorter length within electrochemical cycling. In addition, the evolution of the lattice parameters indicates a solid-phase electrochemical reaction of S/CNTs; no diffraction peaks would be observed if S species were dissolved via a conventional solid–liquid–solid reaction. HRTEM images showing the evolution of S chains inside DWCNTs (Figure S12) confirm that the chains are confined by the CNTs and gradually shorten during electrochemical cycling. Thus, more numerous active terminal S atoms are exposed to Li^+ ions, and the diffusion path for Li^+ ions is reduced. With the chain length reduced after the initial cycle, the reduction peak at 2.0 V increases while the one at 1.45 V decreases (Figure 2c), reflecting improved kinetics. The evolution of the chains implies that they undergo structural self-optimization during electrochemical reactions, ending in an electrochemically preferred structure. Similar phenomena have been reported before.[8,13]

In situ Raman spectra measured during the initial CV further elucidated the structure evolution of S chains during electrochemical reaction (Figures 4d,e). The characteristic Raman peak of S chains (at ~390 nm^{-1}) disappears after the reduction peak at 1.45 V. This demonstrates breaking of the ordered S chains, in agreement with the ex situ XRD results. Raman peaks of Li_2S (Figure S13) were not observed when S chains were reduced to 1.0 V, possibly because the stretching mode of 1D Li_2S is different from that of crystalline Li_2S. When oxidized, S chains break into short ones, in good agreement with the analysis of ex situ XRD results. In addition, the RBM peaks and even the D, G, and 2D bands of CNTs shrink significantly during lithiation, as revealed by the in situ Raman spectra (Figures 4e and S14); delithiation leads to only partial restoration of these peaks. This implies that the spatial confinement in the CNTs is so strong that the Li^+ ions interact intimately with the enclosing C walls.

The spatial confinement also leads to solid-phase diffusion of the Li^+ ions. Because the narrow CNT inner space occupied by S chains can hardly accommodate any solvent molecules, Li^+ ions are desolvated and diffuse through the CNTs as solid-state ions, in contrast to the conventional solid–liquid–solid reaction in most S cathodes.[13] The solid-phase reaction evidenced by the ex

DOI: 10.1021/ja513009v
J. Am. Chem. Soc. 2015, 137, 2215–2218

situ XRD data is considered free from parasitic reactions and dissolution issues,[13] which is advantageous in Li−S batteries, but leads to slow Li^+ diffusion (see Figure S15 for more discussion). As the limited kinetics results from the steric effect, optimizing the host material for shorter S chains would facilitate the (de)lithiation process. This may explain why the S_{2-4} molecules, the shortest S chains, exhibit outstanding electrochemical properties.[5] Intriguingly, in this model system, the S chains can spontaneously become short during cycling, leading to a better electrochemical and kinetic process.

With the well-defined 1D S chains in CNTs as a model system, we studied the electrochemical lithiation/delithiation reaction mechanism of S chains in a Li−S battery (Figure 5). It was found

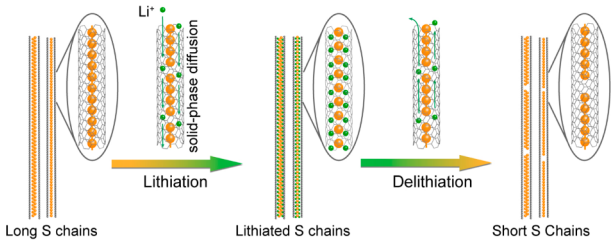

Figure 5. Schematic presentation of proposed electrochemical lithiation/delithiation processes of S chains in a Li−S battery.

that the S chains possess high electrochemical activity, undergo solid-phase electrochemical reactions, and prefer short chain length. The solid-phase reaction is advantageous in Li−S batteries free from dissolution issues but leads to slow kinetics. The kinetics can be improved by utilizing rational nanoporous host materials, such as short cylindrical micropores. The S chains optimize their structure spontaneously during electrochemical reactions (reducing the chain length to ~20 nm) toward better electrochemical performance. The short S chains show improved kinetics and output potentials compared with the long chains as well as superior electrochemical activity. This finding implies that we can design suitable host materials to limit the length of the chains (<20 nm) to improve the electrochemical performance of S chains. S chains in optimized systems are prospective candidates for energy storage applications. Moreover, the electrochemical study of S chains broadens our understanding about the electrochemistry of S beyond S_8 rings, which will provide more opportunities for future S cathodes.

■ ASSOCIATED CONTENT

Supporting Information

Procedures and additional data. This material is available free of charge via the Internet at http://pubs.acs.org.

■ AUTHOR INFORMATION

Corresponding Authors

*ygguo@iccas.ac.cn
*wanlijun@iccas.ac.cn

Notes

The authors declare no competing financial interest.

■ ACKNOWLEDGMENTS

This work was supported by the CAS Strategic Priority Research Program (XDA09010300), the National Natural Science Foundation of China (51225204, U1301244), the National Basic Research Program of China (2011CB935700, 2012CB932900, 2013AA050903), and CAS.

■ REFERENCES

(1) (a) Goodenough, J. B.; Kim, Y. *Chem. Mater.* **2010**, *22*, 587. (b) Zhang, T.; Zhou, H. *Angew. Chem., Int. Ed.* **2012**, *51*, 11062. (c) Abouimrane, A.; Dambournet, D.; Chapman, K. W.; Chupas, P. J.; Weng, W.; Amine, K. *J. Am. Chem. Soc.* **2012**, *134*, 4505. (d) Yang, D.; Lu, Z.; Rui, X.; Huang, X.; Li, H.; Zhu, J.; Zhang, W.; Lam, Y. M.; Hng, H. H.; Zhang, H.; Yan, Q. *Angew. Chem., Int. Ed.* **2014**, *53*, 9352. (e) Dong, S.; Chen, X.; Zhang, X.; Cui, G. *Coord. Chem. Rev.* **2013**, *257*, 1946. (f) Zhou, W.; Cao, X.; Zeng, Z.; Shi, W.; Zhu, Y.; Yan, Q.; Liu, H.; Wang, J.; Zhang, H. *Energy Environ. Sci.* **2013**, *6*, 2216. (g) Sun, G.; Liu, J.; Zhang, X.; Wang, X.; Li, H.; Yu, Y.; Huang, W.; Zhang, H.; Chen, P. *Angew. Chem., Int. Ed.* **2014**, *53*, 12576. (h) Cao, X.; Yin, Z.; Zhang, H. *Energy Environ. Sci.* **2014**, *7*, 1850. (i) Zhu, J.; Yang, D.; Yin, Z.; Yan, Q.; Zhang, H. *Small* **2014**, *10*, 3480.

(2) (a) Rauh, R. D. *J. Electrochem. Soc.* **1979**, *126*, 523. (b) Bruce, P. G.; Freunberger, S. A.; Hardwick, L. J.; Tarascon, J. M. *Nat. Mater.* **2012**, *11*, 19. (c) Xin, S.; Yin, Y.-X.; Guo, Y.-G.; Wan, L.-J. *Adv. Mater.* **2014**, *26*, 1261. (d) Kim, H. S.; Arthur, T. S.; Allred, G. D.; Zajicek, J.; Newman, J. G.; Rodnyansky, A. E.; Oliver, A. G.; Boggess, W. C.; Muldoon, J. *Nat. Commun.* **2011**, *2*, No. 427.

(3) (a) Evers, S.; Nazar, L. F. *Acc. Chem. Res.* **2013**, *46*, 1135. (b) Yin, Y.-X.; Xin, S.; Guo, Y.-G.; Wan, L.-J. *Angew. Chem., Int. Ed.* **2013**, *52*, 13186. (c) Guo, J.; Yang, Z.; Yu, Y.; Abruña, H. D.; Archer, L. A. *J. Am. Chem. Soc.* **2013**, *135*, 763. (d) Xiao, L.; Cao, Y.; Xiao, J.; Schwenzer, B.; Engelhard, M. H.; Saraf, L. V.; Nie, Z.; Exarhos, G. J.; Liu, J. *Adv. Mater.* **2012**, *24*, 1176. (e) Zhang, C.; Wu, H. B.; Yuan, C.; Guo, Z.; Lou, X. W. *Angew. Chem., Int. Ed.* **2012**, *51*, 9592. (f) Hassoun, J.; Scrosati, B. *Adv. Mater.* **2010**, *22*, 5198. (g) Fu, Y.; Zu, C.; Manthiram, A. *J. Am. Chem. Soc.* **2013**, *135*, 18044. (h) Lin, Z.; Liu, Z.; Dudney, N. J.; Liang, C. *ACS Nano* **2013**, *7*, 2829.

(4) (a) Yuan, L.; Qiu, X.; Chen, L.; Zhu, W. *J. Power Sources* **2009**, *189*, 127. (b) Nelson, J.; Misra, S.; Yang, Y.; Jackson, A.; Liu, Y.; Wang, H.; Dai, H.; Andrews, J. C.; Cui, Y.; Toney, M. F. *J. Am. Chem. Soc.* **2012**, *134*, 6337. (c) Feng, X.; Song, M.-K.; Stolte, W. C.; Gardenghi, D.; Zhang, D.; Sun, X.; Zhu, J.; Cairns, E. J.; Guo, J. *Phys. Chem. Chem. Phys.* **2014**, *16*, 16931. (d) Patel, M. U.; Demir-Cakan, R.; Morcrette, M.; Tarascon, J.-M.; Gaberscek, M.; Dominko, R. *ChemSusChem* **2013**, *6*, 1177. (e) Barchasz, C.; Molton, F.; Duboc, C.; Leprêtre, J.-C.; Patoux, S.; Alloin, F. *Anal. Chem.* **2012**, *84*, 3973. (f) Evers, S.; Yim, T.; Nazar, L. F. *J. Phys. Chem. C* **2012**, *116*, 19653.

(5) Xin, S.; Gu, L.; Zhao, N. H.; Yin, Y. X.; Zhou, L. J.; Guo, Y. G.; Wan, L. J. *J. Am. Chem. Soc.* **2012**, *134*, 18510.

(6) Moon, S.; Jung, Y. H.; Jung, W. K.; Jung, D. S.; Choi, J. W.; Kim, D. K. *Adv. Mater.* **2013**, *25*, 6547.

(7) (a) Steudel, R.; Eckert, B. *Top. Curr. Chem.* **2003**, *230*, 1. (b) Meyer, B. *Chem. Rev.* **1976**, *76*, 367. (c) Meyer, B. *Chem. Rev.* **1964**, *64*, 429.

(8) Yang, C.-P.; Xin, S.; Yin, Y.-X.; Ye, H.; Zhang, J.; Guo, Y.-G. *Angew. Chem., Int. Ed.* **2013**, *52*, 8363.

(9) Fujimori, T.; Morelos-Gómez, A.; Zhu, Z.; Muramatsu, H.; Futamura, R.; Urita, K.; Terrones, M.; Hayashi, T.; Endo, M.; Hong, S. Y.; Choi, Y. C.; Tománek, D.; Kaneko, K. *Nat. Commun.* **2013**, *4*, No. 2162.

(10) (a) Guo, J.; Xu, Y.; Wang, C. *Nano Lett.* **2011**, *11*, 4288. (b) Cheng, X.-B.; Huang, J.-Q.; Zhang, Q.; Peng, H.-J.; Zhao, M.-Q.; Wei, F. *Nano Energy* **2014**, *4*, 65.

(11) (a) Rao, A. M.; Richter, E.; Bandow, S.; Chase, B.; Eklund, P. C.; Williams, K. A.; Fang, S.; Subbaswamy, K. R.; Menon, M.; Thess, A.; Smalley, R. E.; Dresselhaus, G.; Dresselhaus, M. S. *Science* **1997**, *275*, 187. (b) Jorio, A.; Pimenta, M. A.; Souza Filho, A. G.; Saito, R.; Dresselhaus, G.; Dresselhaus, M. S. *New J. Phys.* **2003**, *5*, No. 139.

(12) Su, Y.-S.; Fu, Y.; Cochell, T.; Manthiram, A. *Nat. Commun.* **2013**, *4*, No. 2985.

(13) Li, Z.; Yuan, L.; Yi, Z.; Sun, Y.; Liu, Y.; Jiang, Y.; Shen, Y.; Xin, Y.; Zhang, Z.; Huang, Y. *Adv. Energy Mater.* **2014**, *4*, No. 1301473.

DOI: 10.1021/ja513009v
J. Am. Chem. Soc. 2015, 137, 2215−2218